

**Recent progress of redox-responsive polymeric  
nanomaterials for controlled release**

Journal:	<i>Journal of Materials Chemistry B</i>
Manuscript ID	TB-PER-09-2020-002190.R1
Article Type:	Perspective
Date Submitted by the Author:	19-Oct-2020
Complete List of Authors:	Hsu, Peng-Hao; University of California San Diego, Department of Chemistry and Biochemistry Almutairi, Adah; University of California San Diego, Skaggs School of Pharmacy and Pharmaceutical Sciences

## ARTICLE

## Recent progress of redox-responsive polymeric nanomaterials for controlled release

Peng-Hao Hsu <sup>a</sup> and Adah Almutairi <sup>\*b</sup>Received 00th January 20xx,  
Accepted 00th January 20xx

DOI: 10.1039/x0xx00000x

Redox-responsive polymeric nanomaterials (PNMs) have been attractive research targets for drug delivery systems because disturbed levels of redox molecules are associated with the progression of various diseases. To render PNMs targeting biorelevant redox molecules, including reactive oxygen species (ROS), glutathione (GSH) and hydrogen sulfide (H<sub>2</sub>S), appropriate responsive moieties have to be installed within the polymer structure. Upon application of redox stimuli, redox-responsive PNMs undergo structural changes to release encapsulated payloads. Chalcogen ether, thioketal and arylboronic ester have been widely incorporated in the structure of ROS-responsive PNMs. While disulfide is commonly utilized in GSH-responsive PNMs, azide is the newly explored responsive motif targeting H<sub>2</sub>S selectively. Diselenide, on the other hand, is a group susceptible to both oxidative and reducing conditions and therefore exploited in dual redox-responsive PNMs. Here we review PNMs, mainly reported in the recent four years, that contain these redox-responsive moieties for controlled payload release.

### 1. Introduction

Nanometer-sized materials have been appealing tools as drug delivery systems (DDSs) for disease prevention and treatment. In particular, polymeric nanomaterials (PNMs) show the advantage of achieving versatile properties and functions by rationally designing and modulating the structure of the composing polymers and nanoarchitectures. Therefore, the research field of PNMs has been rapidly growing in the past decades.

To enable PNMs to deliver and release therapeutics in a temporally and spatially controlled manner, great efforts have been made to develop stimuli-responsive PNMs. In the presence of applied stimuli, the composing polymers of stimuli-responsive PNMs can undergo physical, chemical or both changes, which subsequently alters the architecture of PNMs and trigger the release of encapsulated therapeutics.<sup>1,2</sup> To further locate release events in the disease sites, disease-relevant stimuli, especially chemical cues in tumor microenvironment (TME), are popular targets of stimuli-responsive PNMs.<sup>3,4</sup> Instead of oxidative phosphorylation, tumor cells obtain energy preferably through glycolysis, which leads to the accumulation of lactate and therefore a lower pH value in TME.<sup>5</sup> To exploit the acidic nature of TME, pH-responsive PNMs have been extensively investigated as DDSs for solid tumors. However, the sensitivity of pH-responsive PNMs has to be finely tuned to ensure that these PNMs show a

sharp response within the pH range observed in TME (6.5–7.2), which is a major challenge in the development of pH-responsive PNMs. On the other hand, TME shows disturbed levels of redox molecules and misregulated redox activities. Given the involvements of biological oxidants and reductants in cellular activities related to tumor development, redox molecules appear as potential targets of stimuli-responsive PNMs. Since the difference between the redox states of healthy tissues and TME is significant, redox-responsive PNMs are promising candidates of DDSs selective for TME.<sup>6–9</sup>

Here we review the current state of redox-responsive PNMs for controlled release based on the responsive groups installed in the polymer structure (Table 1). The discussions start with two major kinds of PNMs that have been investigated considerably: ROS- and GSH-responsive PNMs. We also highlight the development of PNMs that are responsive to H<sub>2</sub>S, a recently explored reductant stimulus. Finally, we review diselenide-based PNMs that are susceptible to both oxidative and reducing conditions.

### 2. ROS-responsive PNMs

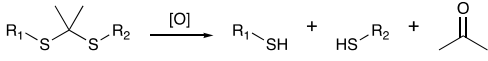
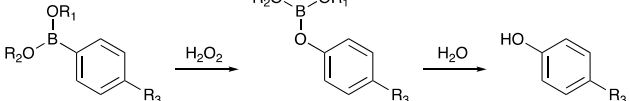
ROS is a group of oxygen-containing molecules including radical species, superoxide (O<sub>2</sub><sup>•-</sup>) and hydroxyl radical (•OH), as well as non-radical species, hydrogen peroxide (H<sub>2</sub>O<sub>2</sub>) and singlet oxygen (<sup>1</sup>O<sub>2</sub>). Since H<sub>2</sub>O<sub>2</sub> has a longer half-life than other ROS, it is the most abundant ROS in eukaryotes, making H<sub>2</sub>O<sub>2</sub> a suitable stimulus target for ROS-responsive PNMs.<sup>10</sup> Indeed, H<sub>2</sub>O<sub>2</sub> is the most commonly used ROS for investigating responsiveness behaviors of ROS-responsive nanomaterials.

Due to the natures of long diffusion distance and the permeability across cell membrane, H<sub>2</sub>O<sub>2</sub> is an important

<sup>a</sup> Department of Chemistry and Biochemistry, University of California San Diego, 9500 Gilman Dr., La Jolla, CA 92093, USA.

<sup>b</sup> Skaggs School of Pharmacy and Pharmaceutical Sciences, University of California San Diego, 9500 Gilman Dr., La Jolla, CA 92093, USA.

**Table 1** Redox-responsive groups and their responsiveness behaviors.

Responsive group	Stimulus target(s)	Responsiveness behavior(s)	References
Chalcogen ether	ROS	$R_1-X-R_2 \xrightarrow{[O]} R_1-\overset{O}{\underset{O}{X}}-R_2 \xrightarrow{[O]} R_1-\overset{O}{\underset{O}{\overset{O}{X}}}-R_2$ X = S, Se and Te	20–22, 25, 26, 32, 33
Thioacetal	ROS		35–40
Arylboronic ester	ROS		42–46
Disulfide	GSH	$R_1-S-S-R_2 \xrightarrow{GSH} R_1-S-SG + HS-R_2$ or $R_1-S-S-R_2 \xrightarrow{GSH} R_1-SH + GS-S-R_2$	63–75
Azide	H <sub>2</sub> S	$R-N_3 \xrightarrow{H_2S} R-NH_2$	94–96
Diselenide	ROS and GSH	$R_1-Se-Se-R_2 \xrightarrow{[O]} R_1-\overset{O}{\underset{O}{Se}}-OH + HO-\overset{O}{\underset{O}{Se}}-R_2$ $R_1-Se-Se-R_2 \xrightarrow{GSH} R_1-SeH + HSe-R_2$	99–101

second messenger in redox signaling.<sup>11</sup> By selectively oxidizing specific cysteine residues, H<sub>2</sub>O<sub>2</sub> regulates activities of several transcriptional factors and thus mediate various cellular processes including cell proliferation, cell differentiation and apoptosis.<sup>12</sup> Endogenous H<sub>2</sub>O<sub>2</sub> is mainly produced from dismutation of superoxide enzymatically or non-enzymatically. Notably, H<sub>2</sub>O<sub>2</sub> is not evenly distributed from extracellular to intracellular spaces. While the concentration of H<sub>2</sub>O<sub>2</sub> in cells ranges between 1–10 nM, the normal level of H<sub>2</sub>O<sub>2</sub> in blood plasma is 1–5 μM.<sup>13</sup> When H<sub>2</sub>O<sub>2</sub> is overproduced or pathways to eliminate H<sub>2</sub>O<sub>2</sub> are disrupted, the resulting abnormally high level of H<sub>2</sub>O<sub>2</sub> (50–100 μM) causes oxidative stress that might contribute to the progression of neurodegenerative diseases, cardiovascular diseases and cancer.<sup>14,15</sup> Considering that various nanomaterials have been widely employed as DDSs or theranostics, the development of ROS-responsive, especially H<sub>2</sub>O<sub>2</sub>-responsive, PNMs might benefit the diagnosis and treatment of diseases associated with oxidative stress. Indeed, this research field has attracted great attention, and there are already several comprehensive reviews about designs and applications of ROS-responsive PNMs.<sup>16–18</sup> Herein we only highlight organochalcogen- and organoboron-based PNMs reported within the last three years. It is noteworthy that vinylthioether-installed PNMs are also responsive to ROS but only selective to <sup>1</sup>O<sub>2</sub>.<sup>19</sup>

### 2.1. Chalcogen ether-based PNMs

Thioether, selenoether and telluroether are sulfur, selenium and tellurium analogs of ether respectively. Because S, Se and Te belong to the same group of the periodic table, these three ether analogs share similar chemical reactivities toward oxidative conditions. Taking thioether as the example, it is oxidized to sulfoxide and further to sulfone in the presence of

oxidants. Considering the increasing hydrophilicity of ether analogs after each stage of oxidation, ROS-triggered hydrophilicity switch is the main responsiveness mechanism employed by thioether-, selenoether- and telluroether-based PNMs.

Thioether is the first functional group employed as the ROS-responsive motif for oxidation-responsive PNMs,<sup>20</sup> and it can be incorporated into the polymer structure either within the main chain, within the pendant groups, or both.<sup>21,22</sup> The resulting thioether-based PNMs showed controlled release of payloads, including fluorescent dye Nile Red (NR) and anticancer drug doxorubicin (DOX). Despite the fact that thioether-containing polymers have been extensively developed for ROS-responsive nanomaterials, thioether-based PNMs show low sensitivity to ROS, limiting their applications in biological systems.<sup>23</sup>

Due to the lower electronegativity of selenium, selenide compounds are more sensitive to oxidative conditions than sulfide compounds.<sup>24</sup> Most selenoether-based PNMs respond to ROS via hydrophilicity switch of the composing polymers.<sup>25,26</sup> Until recently, Yu *et al.* reported a new responsiveness behavior of selenoether-bearing polymers to oxidative conditions.<sup>27</sup> The authors prepared a polycaprolactone (PCL) bearing pendant selenoether motifs at α-positions of ester moieties. Once the pendant selenoether is oxidized, the resulting selenoxide undergoes an internal *syn* elimination to generate an α,β-unsaturated carbonyl moiety on the polymer backbone and release the pendant selenenic acid fragment. While such tandem processes of oxidation and selenoxide elimination can induce C–Se bond breakages on the pendant groups, the polymer backbone does not undergo ROS-responsive degradation. Inspired by this work, Xu's group designed and synthesized another polymer that responds to ROS through selenoxide elimination reactions.<sup>28,29</sup> This polymer bears β-

selenylated dicarbonyl moieties on the polymer main chain. Upon oxidation, the selenoxide moieties undergo *syn* eliminations to scissor the backbone into short fragments. The authors also demonstrated that acrylate fragments generated from polymer degradation have an additional anticancer effect by depleting intracellular GSH and disturbing the redox balance. This new degradable selenoether-based polymer shows promising future applications for ROS-controlled drug release.

In contrast to sulfur and selenium, tellurium has the lowest electronegativity, indicating that the sensitivity of telluride compounds to oxidative conditions is even higher than selenide and sulfide compounds.<sup>30,31</sup> Xu's group has investigated the ROS-responsive behaviors of telluroether-based PNMs and found that tellurium-containing PNMs are sensitive to not only biologically relevant concentrations of H<sub>2</sub>O<sub>2</sub> but also trace amount of ROS generated by  $\gamma$ -ray irradiation.<sup>32</sup> Following these pioneering studies, Fan *et al.* fabricated nanoparticles (NPs) from a diblock amphiphilic polymer consisting a polyethylene glycol (PEG) block and a hydrophobic block bearing pendant telluroether groups (Figure 1).<sup>33</sup> The coordination capability of tellurium with the platinum center of cisplatin facilitates the encapsulation of cisplatin during NP self-assembly. Upon  $\gamma$ -ray irradiation, trace ROS generated in aqueous solutions oxidizes telluroether moieties to weaken the coordination of tellurium with cisplatin and thus result in the release of cisplatin from NPs. These results suggest the potential of telluroether-based PNMs as nanoplatforms for both chemo- and radio-therapies. On the other hand,  $\beta$ -telluro diesters, when installed within the polymer main chain, also exhibits ROS-induced backbone degradation via *syn* eliminations of telluroxide moieties.<sup>28</sup> Compared to  $\beta$ -selenylated dicarbonyl moiety,  $\beta$ -telluro diester exhibited higher sensitivity to ROS, suggesting future applications of this group as responsive units of ultrasensitive ROS-responsive PNMs.

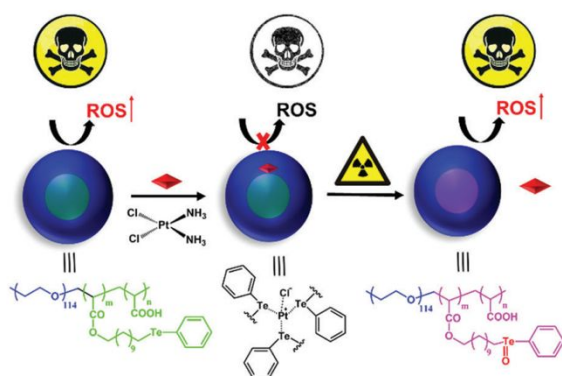


**Figure 1** ROS-induced release of cisplatin from telluroether-based NPs upon  $\gamma$ -ray irradiation. Reproduced from Ref. 33 with permission from The Royal Society of Chemistry.

## 2.2. Thioketal-based PNMs

Similar to thioether, thioketal is a sulfur-based ROS-responsive group, and it has been shown to react with a broad spectrum of ROS including H<sub>2</sub>O<sub>2</sub>, superoxide, hydroxyl radical and hypochlorite.<sup>34</sup> However, in contrast to nondegradable

thioether, thioketal linkage dissociates to release two thiol fragments and one molecule of acetone upon oxidation. Therefore, thioketal-based PNMs respond to ROS via hydrophilicity switch or backbone cleavage induced by scissions of thioketal linkages.

When thioketal moieties are incorporated in the polymer main chain, the presence of ROS can directly induce polymer degradation and thus dissociation of PNMs. Xu *et al.* has adopted this strategy to prepare two thioketal-containing copolymers, mPEG-poly(thioketal-ester) and mPEG-poly(thioketal-ester-thioether), as well as the other copolymer, mPEG-poly(ester-thioether).<sup>35</sup> The authors then compared the ROS-responsive behaviors of three different NPs formulated from these amphiphilic copolymers respectively. Based on the results, DOX-loaded mPEG-poly(ester-thioether) NPs showed the fastest ROS-induced drug release and the highest *in vitro* anticancer activity, suggesting that thioketal-based PNMs might suffer the issue of a lower sensitivity to ROS. Thioketal can be also exploited to interconnect polyethylenimine or oligoethylenimine.<sup>36,37</sup> The resulting thioketal-containing cationic polymers have been developed for ROS-responsive gene delivery.

On the other hand, thioketal linkers have been employed in the pendant groups to graft drugs on polymer backbones for polyprodrug preparations. To achieve a more efficient thioketal cleavage and the subsequent drug release, nanoformulations of thioketal-based polyprodrugs were coupled with ROS generators. The co-delivered ROS generator can also pose an oxidative stress to cancer cells and therefore exert an additional anticancer effect. Pei *et al.* prepared chlorin e6 (Ce6)-encapsulated NPs from a polyphosphoester bearing thioketal-linked DOX.<sup>38</sup> Upon red light irradiation, ROS generated from the photosensitizer Ce6 could induce DOX release and NP disassembly. Considering the penetration limit of exogenous light used for photosensitizer, Zhang *et al.* utilized a self-circulating amplification approach.<sup>39</sup> The authors formulated NPs from two amphiphilic polyprodrugs bearing two different terminal ligands, which target cancer cells and mitochondria respectively, and a common hydrophobic block with pendant thioketal-linked camptothecin (CPT). Once the NPs are internalized into mitochondria, endogenous mitochondrial ROS induces the breakage of thioketal linkers to release CPT. The free CPT can further trigger ROS production and result in a self-circulating amplification of CPT release and ROS burst. Wang *et al.* prepared NPs from the co-assembly of an acid-sensitive polymer and a polyprodrug of DOX in the presence of  $\beta$ -lapachone and iron ion (Figure 2).<sup>40</sup> When these NPs accumulate in TME, the acidic environment induces NP disassembly and payload release via protonating tertiary amine moieties on the acid-sensitive polymer. Once  $\beta$ -lapachone and iron ion are released, the enzyme-catalyzed generation of H<sub>2</sub>O<sub>2</sub> from  $\beta$ -lapachone and the subsequent production of hydroxyl radical from H<sub>2</sub>O<sub>2</sub> through the Fenton reaction can exert antitumor effect and help to scissor ketal linkages on polyprodrugs to release DOX. This strategy combines chemotherapy and chemodynamic therapy to enhance antitumor efficacy.

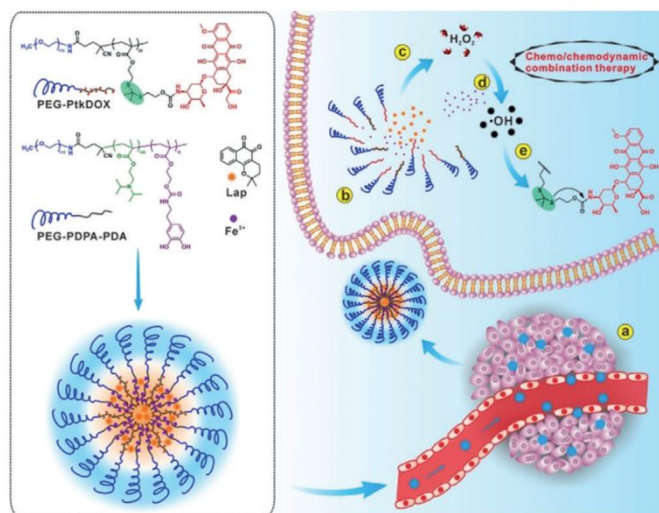


**Figure 2** Schematic illustration of the strategy combining chemodynamic therapy and chemotherapy. Reproduced from Ref. 40 with permission from John Wiley & Sons.

### 2.3. Arylboronic ester-based PNMs

Arylboronic ester is another common ROS-responsive functional group. Due to its high selectivity and sensitivity to  $H_2O_2$  but other ROS species, arylboronic ester moieties have been widely employed in  $H_2O_2$ -responsive fluorescent probes and nanomaterials. The reaction between arylboronic ester and  $H_2O_2$  involves several steps including the nucleophilic addition of  $H_2O_2$  to the boron center, the migration of the aryl group to the oxygen atom via a 1,2-insertion and the final hydrolysis of the borate ester to release phenol. The phenol species might undergo an additional 1,4- or 1,6-rearrangement to further expose the group originally capped with arylboronic ester. To install arylboronic ester moieties within the polymer structure, these groups are usually introduced as pendant groups on the polymer backbone. Such arylboronic ester-bearing polymers respond to  $H_2O_2$  mainly through two mechanisms: backbone breakage or hydrophilicity switch.<sup>41</sup>

Our group has synthesized two ROS-responsive polymers using pendant arylboronic ester moieties to mask reactive groups that can scissor the polymer backbone. ROS-ARP is a polymer containing ketal functionalities in the backbone and pendant arylboronic ester-masked carboxylic acids.<sup>42</sup> Upon uncapping the arylboronic ester moieties with  $H_2O_2$ , the revealed carboxylic acids catalyze the hydrolysis of local ketal functionalities and therefore result in backbone breakage. This chemical amplification approach was shown to effectively accelerate  $H_2O_2$ -induced depolymerization up to 17-fold compared to a ROS-responsive control polymer, but NPs prepared from ROS-ARP are not sensitive enough to exhibit significant release of IR-780 in response to biologically relevant levels of  $H_2O_2$ . To improve the sensitivity of ROS-responsive PNMs, we synthesized another polymer called oxidation-responsive PCL (O-PCL), on which arylboronic ester moieties were used to mask pendant amino groups (Figure 3).<sup>43</sup> In the presence of  $H_2O_2$ , the oxidation of arylboronic ester and the following 1,6-rearrangement expose amino groups that can

undergo intramolecular cyclization to break ester linkages on the polymer backbone. Due to the fast kinetics of intramolecular cyclization, O-PCL showed rapid  $H_2O_2$ -induced depolymerization. Besides, NPs formulated from O-PCL released encapsulated superparamagnetic iron oxide nanoparticles in response to  $50 \mu M$  of  $H_2O_2$ , indicating the high sensitivity of O-PCL to disease relevant concentrations of  $H_2O_2$ .

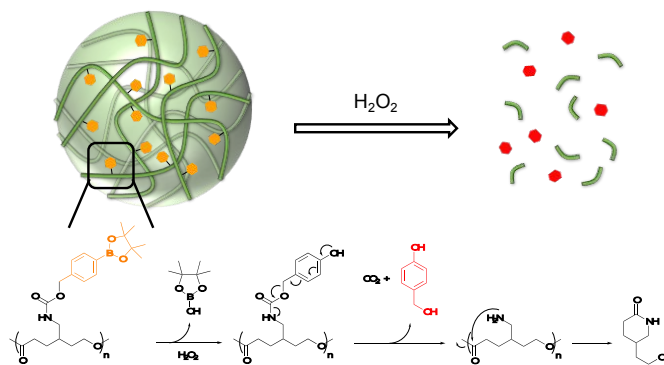


**Figure 3** Schematic illustration of  $H_2O_2$ -induced degradation of O-PCL. Reproduced from Ref. 43 with permission from The Royal Society of Chemistry.

When hydrophilicity switch is employed as the responsiveness mechanism, grafting hydrophobic arylboronic ester moieties on a hydrophilic polymer main chain or polymer block is a feasible and common approach to prepare a ROS-responsive polymer. Our group synthesized an oxidation-responsive dextran-based polyprodrug, Nap-Dex, by conjugating anti-inflammatory drug naproxen on dextran through boronic ester linkages.<sup>44</sup>  $H_2O_2$  induced the dissociation of naproxen from dextran and thus a hydrophilicity switch of the polymer backbone. By blending Nap-Dex with acetalated dextran, we formulated NPs that could release naproxen to reduce the levels of IL-6 and TNF $\alpha$  under inflammatory conditions. Instead of directly conjugating arylboronic ester moieties on a natural polymer, Jäger *et al.* synthesized a diblock copolymer that bears pendant arylboronic ester-masked carboxylic acids on the hydrophobic block.<sup>45</sup> After incubating with  $H_2O_2$ , this copolymer showed a hydrophilicity switch due to the liberation of arylboronic ester moieties to reveal carboxylic acids. The polymersomes assembled from this diblock copolymer were used to deliver DOX to TME to exert anticancer effects. Utilizing a similar responsiveness strategy, Garcia *et al.* prepared another diblock copolymer containing an arylboronic ester-functionalized hydrophobic polycarbonate block and a hydrophilic PEG block. The authors then investigated  $H_2O_2$ -induced disassembly behaviors of NPs formulated from this copolymer.<sup>46</sup> Their results showed that the release rate of NR is related to concentrations of  $H_2O_2$  while the rate of NP disassembly depends on not only the concentrations of  $H_2O_2$  but also the polymer concentration, which poses another consideration when examining responsiveness behaviors of stimuli-responsive PNMs.

### 3. GSH-responsive PNMs

GSH, a tripeptide consisting of glutamate, cysteine and glycine, is the most abundant intracellular small molecule biothiol.<sup>47</sup> Due to its capability of switching between the reduced thiol state (GSH) and the oxidized disulfide state (GSSG) through enzymatic reactions, GSH has functions of antioxidation and detoxification, and thus mediates several cellular processes, including redox homeostasis, apoptosis, cellular proliferation and differentiation.<sup>48–51</sup> GSH is produced by two consecutive enzymatic reactions catalyzed by glutamate-cysteine ligase (GCL) and glutathione synthetase. One important feature of GSH is that it distributes unevenly within human bodies. The intracellular GSH concentration (1–10 mM) is significantly higher than the extracellular GSH concentration (1–10  $\mu$ M),<sup>52</sup> which makes GSH an ideal stimulus target for intracellular delivery. Given that ROS is overproduced in cancer tissues, certain cancer tissues, such as breast and lung cancers, express elevated levels of GCL to overproduce GSH<sup>53–56</sup> to counteract the oxidative stress posed by ROS and maintain the redox balance.<sup>57–59</sup> Therefore, GSH-responsive PNMs show promising applications as intracellular DDSs for cancer cells.<sup>8,52,59</sup>

### 3.1. Disulfide-based PNMs

Disulfide bond is the most common moiety exploited for GSH-responsive PNM due to its capability of undergoing thiol–disulfide exchange reaction with free thiols.<sup>60</sup> The abnormally high concentrations of GSH in cancer tissues can disintegrate nanomaterial structures that were held by disulfide bonds through this thiol–disulfide exchange reaction. GSH-responsive disulfide-based PNMs can be broadly divided into three groups based on where disulfide bonds are installed: within the polymer main chain, within the pendant groups and within the cross-linker.<sup>61</sup> Due to the high volume of the publications about disulfide-based PNMs,<sup>62</sup> we only highlight selected research works published after 2018.

Bawa *et al.* incorporated disulfide bonds within the backbone of a triblock copolymer by using them to connect two hydrophilic blocks with the central hydrophobic block.<sup>63</sup> In addition, they introduced a ketal moiety within the hydrophobic block. Despite this copolymer is functionalized with GSH-responsive groups, the micelles prepared from this polymer showed no significant NR release under reducing conditions presumably because GSH only induced the shedding of the shell but the disintegration of the core. The NR release behavior was, however, observed in a more acidic environment containing GSH. To enhance the responsiveness of disulfide-based nanomaterials, multi-disulfide linkages can be installed within the polymer backbone. Ju *et al.* synthesized a triblock copolymer, PEEP-PDS-PEEP, composed of two hydrophilic poly(ethyl ethylene phosphate) (PEEP) blocks and one hydrophobic poly(disulfide) (PDS) block.<sup>64</sup> The DOX-encapsulated PEEP-PDS-PEEP NPs showed GSH-induced drug release to inhibit cancer cell proliferation.

When disulfide bonds are within the pendant groups, the degradation of GSH-responsive PNMs mainly relies on hydrophilicity switch of the polymer backbone upon GSH-

induced dissociation of pendant hydrophobic groups. Hu *et al.* installed octadecyl groups and iRGD moieties on hydroxyethyl starch through disulfide bonds.<sup>65</sup> The incorporation of octadecyl group facilitates nanocluster formation by hydrophobic interactions, and the introduction of iRGD groups improves nanocluster uptake by cancer cells through the interaction between iRGD and integrin  $\alpha_v$ , a membrane protein associated with tumor growth and metastasis. Once nanoclusters are internalized by cancer cells, intracellular reducing environment triggers the dissociation of octadecyl groups and thus the disintegration of nanoclusters as well as the release of DOX. Besides alkyl chains, hydrophobic small molecule drugs can be also used as pendant groups to provide hydrophobic interactions required for self-assembling process. Several polyprodrugs have been synthesized by incorporating various drugs, such as CPT,<sup>66</sup> chlorambucil<sup>67</sup> and indomethacin,<sup>68</sup> to the polymer backbones using disulfide linkages. Upon treatment with GSH, the dissociation of hydrophobic drug moieties induces not only the degradation of self-assembled nanostructures but also the release of drugs. While disulfide-based polyprodrugs are promising candidates as GSH-responsive DDSs with high drug loading, appropriate disulfide linkers have to be utilized to ensure the release of parent drugs. In addition, the morphology of PNMs should be considered to achieve better cellular internalization.<sup>69</sup> Given the benefits of combined therapy to treat drug-resistant cancers,<sup>70</sup> the co-delivery of a second drug with the polyprodrug has also been exploited. Shen *et al.* synthesized self-assembled NPs from an amphiphilic copolymer bearing pendant disulfide-linked CPT (Figure 4).<sup>71</sup> The encapsulation of DOX within these NPs enables controlled co-releases of two anticancer drugs, DOX and CPT, to exhibit a better inhibitory effect to cancer cells via a synergistic effect.

The third approach to prepare GSH-responsive PNMs is using disulfide-based cross-linkers to covalently link individual polymer chains. In contrast to self-assembled nanostructures hold by non-covalent interactions, physically cross-linked nanomaterials have the advantage of higher colloid stability. Several reactions have been exploited to connect disulfide-based cross-linkers to pre-synthesized polymer chains. Biswas *et al.* utilized bis(acryloyl)cystamine to cross-link oxime-functionalized polymers via isoxazoline formation through a copper-free 1,3-dipolar cycloaddition reaction.<sup>72</sup> Bhattacharya *et al.* applied Diels–Alder reaction to cross-link polymers with pendant furan groups using dithiobismaleimidoethane cross-linkers.<sup>73</sup> In both two reports, covalently cross-linked NGs showed GSH-controlled release of DOX. Li *et al.* formulated polyprodrug micelles from a polymer bearing a disulfide bond connecting the hydrophilic block and the hydrophobic block with pendant DOX groups.<sup>74</sup> The authors further cross-linked the shell of micelle via disulfide-containing dihydrazide linkers to enhance micelle stability and prevent drug leaking. The presence of GSH triggered an increase in micelle size and the release of DOX. Interestingly, Zhao *et al.* directly polymerized methacrylic acid with bis(acryloyl) disulfide linker in the presence of a template, *S*-propranolol.<sup>75</sup> The resulting molecularly imprinted NGs showed higher loading capacity of *S*-

propranolol than the NGs polymerized without the template. In addition, this imprinted NGs exhibited less uncontrolled release of *S*-propranolol. This work might provide an alternative strategy to improve the drug loading capacity of redox-responsive PNMs.

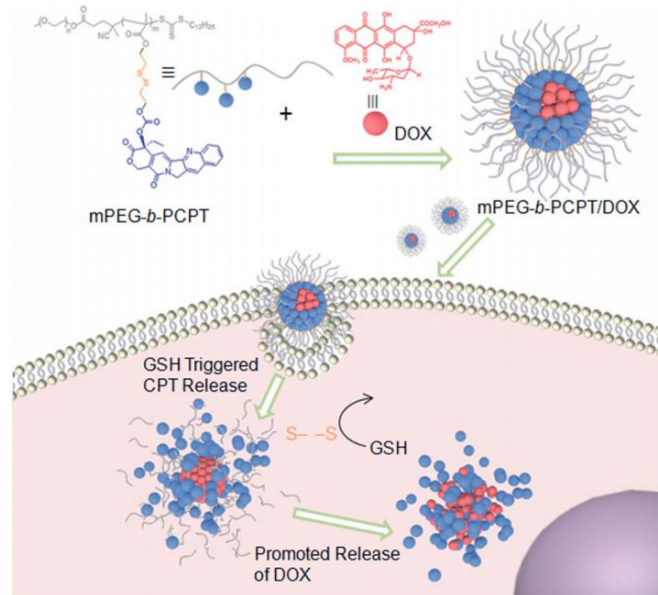


**Figure 4** GSH-induced release of disulfide-linked CPT and physically loaded DOX from polyprodrug NPs. Reproduced from Ref. 71 with permission from The Royal Society of Chemistry.

## 4. H<sub>2</sub>S-responsive PNMs

H<sub>2</sub>S is the simplest gaseous thiol with the smell of rotten eggs. Due to the weakly acidic nature ( $pK_{a1} = 6.98$  at 25 °C and 6.76 at 37 °C),<sup>76</sup> H<sub>2</sub>S mainly exists in the form of deprotonated anion, HS<sup>-</sup>, at neutral conditions, which renders H<sub>2</sub>S both reducing and nucleophilic in biological systems. Although H<sub>2</sub>S had been recognized as a merely toxic substance for a long time, the field of H<sub>2</sub>S biology has received increasing interests in the last decade.<sup>77</sup> H<sub>2</sub>S has been shown to play regulatory roles in the nervous system and the cardiovascular system as well as elicit both proinflammatory and anti-inflammatory effects.<sup>78,79</sup> In the molecular level, H<sub>2</sub>S exerts its effects by protein persulfidation, binding to metal centers of metalloproteins as well as cross-talk with ROS and reactive nitrogen species.<sup>80</sup>

Endogenous H<sub>2</sub>S is produced mainly by three enzymes: cystathionine  $\beta$ -synthase (CBS), cystathionine  $\gamma$ -lyase (CSE), and 3-mercaptopyruvate sulfurtransferase. Physiological levels of H<sub>2</sub>S in the blood of mammals are in the range of 30–100  $\mu$ M while the concentration of H<sub>2</sub>S can reach up to 3.4 mM in human colon.<sup>81,82</sup> Abnormal expression of aforementioned enzymes and thereby misregulated H<sub>2</sub>S production is associated with the progressions of various diseases.<sup>83</sup> Decreased level of H<sub>2</sub>S has been observed in neurodegenerative disorders, such as Huntington's and Alzheimer's diseases,<sup>84</sup> as well as cardiovascular diseases, such as coronary heart disease and

heart failure.<sup>85,86</sup> Notably, although there is no consistent trend of expression levels of H<sub>2</sub>S-producing enzymes among all types of cancer cells, upregulation of CBS and the resulting elevated level of H<sub>2</sub>S has been found in colon, ovarian and breast cancer cells,<sup>87,88</sup> suggesting the potential applications of H<sub>2</sub>S-responsive PNMs as DDSs selective to colon and ovarian cancers. Besides PNMs, there are other nanomaterials, including protein nanocomposites and mesoporous silica nanoparticles, reported to exhibit H<sub>2</sub>S-induced payload release.<sup>89,90</sup>

### 4.1. Azide-based PNMs

Due to emerging evidences of physiological and pathological effects of H<sub>2</sub>S, the research fields of H<sub>2</sub>S-selective imaging and therapeutic agents have also developed rapidly.<sup>91,92</sup> Two organic reaction mechanisms, azide reduction and nucleophilic substitution, are widely utilized in the design of H<sub>2</sub>S-responsive moieties within these H<sub>2</sub>S-selective agents. In particular, the bioorthogonal azido group is highly selective for H<sub>2</sub>S over other biologically relevant thiol species such as GSH and cysteine. Therefore, azide reduction is the only mechanism employed by H<sub>2</sub>S-responsive PNMs to date. In addition, the mechanism of H<sub>2</sub>S-mediated reduction of aryl azide was already well investigated.<sup>93</sup>

The first H<sub>2</sub>S-responsive PNM was reported in 2016. Yan *et al.* synthesized a diblock copolymer, PEO-*b*-PAGMA, consisting of a hydrophilic poly(ethylene oxide) (PEO) block and a hydrophobic poly(*o*-azidomethyl benzoyl glycerol methacrylate) (PAGMA) block (Figure 5).<sup>94</sup> This amphiphilic PEO-*b*-PAGMA spontaneously aggregated to form polymersomes in aqueous solutions. In the presence of H<sub>2</sub>S, reduction of azide to amine initiates intramolecular cyclization to sever hydrophobic side chains from the PAGMA block, resulting in hydrophilicity switch of the hydrophobic block and eventually polymersome disassembly. In addition, the authors encapsulated CSE in the lipid bilayer membrane of PEO-*b*-PAGMA polymersomes. Due to the capability of CSE to produce H<sub>2</sub>S from cysteine, these CSE-anchored polymersomes disassembled and released epinephrine in response to not only H<sub>2</sub>S but also cysteine.

Zhang *et al.* prepared another diblock copolymer, N<sub>3</sub>-Nap-PHEMA-*b*-PMMA-N<sub>3</sub>, composed of a hydrophilic poly(2-hydroxyethyl methacrylate) (PHEMA) block and a hydrophobic poly(methyl methacrylate) (PMMA) block.<sup>95</sup> This copolymer bears an additional aryl azide-based fluorescent probe (N<sub>3</sub>-Nap) at the terminus of the PHEMA block. Upon H<sub>2</sub>S-mediated reduction of N<sub>3</sub>-Nap to NH<sub>2</sub>-Nap, micelle formulated from N<sub>3</sub>-Nap-PHEMA-*b*-PMMA-N<sub>3</sub> showed a turn-on fluorescence and a surface charge reversal to become positively charged, which facilitates cellular internalization of the micelle probe. However, H<sub>2</sub>S-mediated charge reversal itself could not trigger significant amount of DOX release from these micelles. An environment with a lower pH value was also required to achieve an efficient release of DOX.

Besides nanomaterials formulated from synthetic copolymers, our group demonstrated the first H<sub>2</sub>S-responsive

NG.<sup>96</sup> We synthesized a H<sub>2</sub>S-responsive cholesterol-modified dextran (SC-Dex) by grafting cholesteryl groups on biocompatible dextran using aryl azide-based self-immolative linkers. The resulting amphiphilic SC-Dex self-assembled to form NGs via hydrophobic interactions between cholesteryl substitutions. After SC-Dex NGs were incubated with H<sub>2</sub>S, the aryl azide on the self-immolative linker of SC-Dex was reduced to aniline, which initiated 1,4-rearrangement to liberate cholesterol from the dextran backbone and eventually resulted in NG swelling. Notably, the responsiveness behavior of SC-Dex is selective for H<sub>2</sub>S over another abundant biothiol GSH. In addition, SC-Dex NGs were able to encapsulate protein and show controlled payload release in response to H<sub>2</sub>S. This new NG show potential future applications as H<sub>2</sub>S-responsive DDSs of small molecule drugs and biomacromolecules to disease tissues with upregulated H<sub>2</sub>S levels.

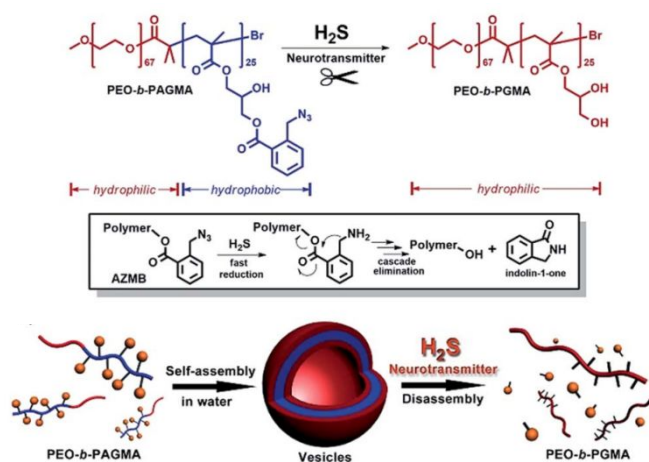


**Figure 5** Schematic illustration of H<sub>2</sub>S-induced hydrophilicity switch of PEO-*b*-PAGMA and disassembly of PEO-*b*-PAGMA polymersomes. Reproduced from Ref. 94 with permission from The Royal Society of Chemistry.

## 5. ROS and GSH dual-responsive PNMs

We have so far reviewed PNMs bearing functional groups that target either oxidative or reducing stimuli. However, there are dual-responsive groups that can react with both ROS and GSH. When PNMs are incorporated with these groups, the resulting PNMs are capable of responding to both oxidative and reducing conditions and show broader applications to more diverse physiological and pathological environments.

Herein we only highlight the development of diselenide-based PNMs because diselenide is the most widely utilized dual-responsive group. It is noteworthy that  $\alpha$ -dicarbonyl thioether has also exploited as the responsive group for the preparation of dual redox-responsive PNMs.<sup>97</sup>

### 5.1. Diselenide-based PNMs

Diselenide bond is well known for its special reactivities to both oxidative and reducing conditions and has been incorporated in the structures of various dual redox-responsive

PNMs. While diselenide bond can be cleaved and oxidized to two seleninic acid units by oxidants, it can also be reduced to two selenol units in the presence of reductants. In addition, diselenide bond is  $\gamma$ -radiation-responsive because it can react with oxidative species formed in the aqueous solution upon  $\gamma$ -radiation.<sup>24,98</sup>

Two common strategies to prepare diselenide-based PNMs are installing diselenide bonds into the polymer main chain and using diselenide-containing structures to cross-link polymer chains. Hailemeskel *et al.* employed the first strategy and synthesized a diselenide-based polymer, (PEGSeSe)<sub>n</sub>, by connecting PEG units with diselenide linkages.<sup>99</sup> The NGs formulated from (PEGSeSe)<sub>n</sub> showed controlled release of DOX in response to GSH, H<sub>2</sub>O<sub>2</sub> and  $\gamma$ -radiation. On the other hand, Tian *et al.* applied the second strategy and fabricated another diselenide-based zwitterionic NGs by copolymerizing 2-methacryloyloxyethyl phosphorylcholine (MPC) with cross-linker *N,N'*-bis(methacryloyl) selenocystamine (BMASC) (Figure 6).<sup>100</sup> Upon treatment with GSH or H<sub>2</sub>O<sub>2</sub>, the cleavage of BMASC induced NG disassembly and DOX release. The zwitterionic nature of these NGs also contributes to lower non-specific protein adsorption and longer blood circulation time.

Given that selenide and sulfur are within the same VI main group, diselenide and disulfide bonds should share similar chemical properties. Zhang *et al.* examined the difference in redox sensitivity between two micelles formulated from two triblock copolymers, mPEG-PCL-SeSe-PCL-mPEG and mPEG-PCL-SS-PCL-mPEG, respectively.<sup>101</sup> The difference between these two copolymers is the linkage, diselenide or disulfide bond, to connect two PCL fragments within the hydrophobic block. The authors observed that diselenide-based micelles showed more and faster DOX release in both reductive and oxidative environments. The higher sensitivity of diselenide-based micelles to both H<sub>2</sub>O<sub>2</sub> and GSH can be explained by the fact that the bond energy of Se–Se (172 kJ/mol) is lower than that of S–S (240 kJ/mol). However, diselenide-based micelles suffer the issue of higher uncontrolled release presumably due to the high sensitivity of Se–Se bond to trace oxidative species present in aqueous solutions.

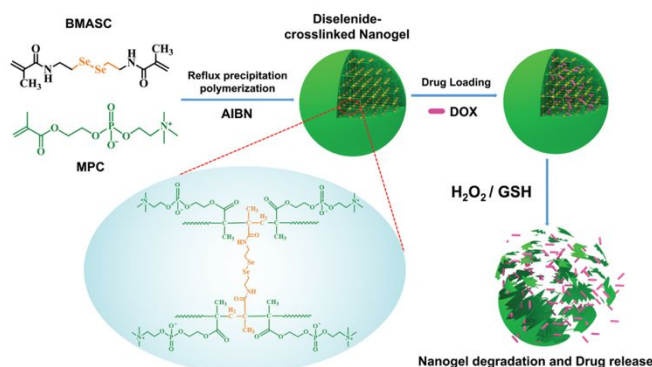


**Figure 6** Schematic illustration of preparation and dual responsive degradation of diselenide-based zwitterionic NGs. Reproduced from Ref. 100 with permission from The Royal Society of Chemistry.

## 6. Conclusions

The use of redox-responsive PNMs as DDSs has been investigated considerably due to the identification of redox imbalance in a variety of diseases, especially in TME. In the past decades, efforts have been made to advance various ROS-responsive PNMs containing organochalcogen or organoboron, GSH-responsive PNMs containing disulfide as well as ROS and GSH dual-responsive PNMs containing diselenide. Recently, the recognition of H<sub>2</sub>S as a new disease marker also brings up the development of H<sub>2</sub>S-responsive PNMs. In this perspective, we cover the latest research of these redox-responsive PNMs.

Despite the flourishing development of new redox-responsive PNMs, the ultimate goal to adopt these materials for clinical uses is still hard to achieve. One important prerequisite for the clinical applicability of redox-responsive PNMs is whether they are sensitive to biorelevant concentrations of redox stimuli. Based on reported comparisons of release behaviors between different ROS-responsive PNMs, the ROS sensitivity of organochalcogen-based groups follows the order of selenoether > diselenide ≈ thioether > thioketal.<sup>35,102</sup> While there is no direct comparison of ROS sensitivity between arylboronic ester and organochalcogen, PNMs bearing arylboronic ester moieties have been shown to respond to biologically relevant levels of H<sub>2</sub>O<sub>2</sub>. In this regard, telluroether, which is even more sensitive to ROS than selenoether, and arylboronic ester are better candidates of ROS-responsive groups due to their high sensitivities to low concentrations of ROS, such as 50–100 μM of H<sub>2</sub>O<sub>2</sub>, observed in disease conditions. The co-delivery of ROS inducer or generator within ROS-responsive PNMs might be another feasible approach to enhance the sensitivity of nanomaterials containing other ROS-responsive groups. On the other hand, considering the biologically relevant levels of GSH and H<sub>2</sub>S can reach the micromolar range, both disulfide and azide are suitable groups for reduction-responsive PNMs.

In addition to explore new responsive groups with higher sensitivity, developing redox-responsive PNMs as multifunctional nanoplatfoms can also expand their biomedical applications. Redox-responsive PNMs can serve as smart nanotheranostics when imaging agents are co-encapsulated or covalently attached to the nanostructure. The capability of redox-responsive theranostics to distinguish TME from healthy tissues further benefits their uses for imaging-guided cancer therapy.<sup>103,104</sup> With improvements of multifunctionality introduction and sensitivity enhancement, redox-responsive PNMs can be promising tools to treat cancer in a more precise and personalized manner.

## Conflicts of interest

The authors declare no competing financial interest.

## Acknowledgements

The authors thank the Air Force office of Scientific Research (AFOSR), FA9550-15-1-0273, for funding.

## Notes and references

- M. Wei, Y. Gao, X. Li and M. J. Serpe, *Polym. Chem.*, 2017, **8**, 127–143.
- J. Zhang, X. Jiang, X. Wen, Q. Xu, H. Zeng, Y. Zhao, M. Liu, Z. Wang, X. Hu and Y. Wang, *J. Phys. Mater.*, 2019, **2**, 032004.
- H. S. El-Sawy, A. M. Al-Abd, T. A. Ahmed, K. M. El-Say and V. P. Torchilin, *ACS Nano*, 2018, **12**, 10636–10664.
- M. Liu, H. Du, W. Zhang and G. Zhai, *Mater. Sci. Eng. C*, 2017, **71**, 1267–1280.
- M. Jin and W. Jin, *Sig. Transduct. Target. Ther.*, 2020, **5**, 166.
- M. Huo, Y. Yuan, L. Tao and Y. Wei, *Polym. Chem.*, 2014, **5**, 1519–1528.
- X. Zhang, L. Han, M. Liu, K. Wang, L. Tao, Q. Wan and Y. Wei, *Mater. Chem. Front.*, 2017, **1**, 807–822.
- X. Guo, Y. Cheng, X. Zhao, Y. Luo, J. Chen and W.-E. Yuan, *J. Nanobiotechnol.*, 2018, **16**, 74.
- A. Raza, U. Hayat, T. Rasheed, M. Bilal and H. M. N. Iqbal, *Eur. J. Med. Chem.*, 2018, **157**, 705–715.
- S. Parvez, M. J. C. Long, J. R. Poganik and Y. Aye, *Chem. Rev.*, 2018, **118**, 8798–8888.
- B. Yang, Y. Chen and J. Shi, *Chem. Rev.*, 2019, **119**, 4881–4985.
- H. S. Marinho, C. Real, L. Cyrne, H. Soares and F. Antunes, *Redox Biol.*, 2014, **2**, 535–562.
- H. Sies, *Redox Biol.*, 2017, **11**, 613–619.
- H. Kong and N. S. Chandel, *J. Biol. Chem.*, 2018, **293**, 7499–7507.
- I. Liguori, G. Russo, F. Curcio, G. Bulli, L. Aran, D. Della-Morte, G. Gargiulo, G. Testa, F. Cacciatore, D. Bonaduce and P. Abete, *Clin. Interv. Aging*, 2018, **13**, 757–772.
- G. Saravanakumar, J. Kim and W. J. Kim, *Adv. Sci.*, 2017, **4**, 1600124.
- H. Ye, Y. Zhou, X. Liu, Y. Chen, S. Duan, R. Zhu, Y. Liu and L. Yin, *Biomacromolecules*, 2019, **20**, 2441–2463.
- F. El-Mohtadi, R. d'Arcy and N. Tirelli, *Macromol. Rapid Commun.*, 2019, **40**, 1800699.
- Z. Liu, T. Cao, Y. Xue, M. Li, M. Wu, J. W. Engle, Q. He, W. Cai, M. Lan and W. Zhang, *Angew. Chem. Int. Ed.*, 2020, **59**, 3711–3717.
- A. Napoli, M. Valentini, N. Tirelli, M. Müller and J. A. Hubbell, *Nat. Mater.*, 2004, **3**, 183–189.
- B. Yan, Y. Zhang, C. Wei and Y. Xu, *Polym. Chem.*, 2018, **9**, 904–911.
- G. Wang, P. Huang, M. Qi, C. Li, W. Fan, Y. Zhou, R. Zhang, W. Huang and D. Yan, *ACS Omega*, 2019, **4**, 17600–17606.
- Z. Fan and H. Xu, *Polym. Rev.*, 2020, **60**, 114–143.
- J. Xia, T. Li, C. Lu and H. Xu, *Macromolecules*, 2018, **51**, 7435–7455.
- N. Ma, Y. Li, H. Ren, H. Xu, Z. Li and X. Zhang, *Polym. Chem.*, 2010, **1**, 1609–1614.
- H. Ren, Y. Wu, N. Ma, H. Xu and X. Zhang, *Soft Matter*, 2012, **8**, 1460–1466.
- L. Yu, M. Zhang, F.-S. Du and Z.-C. Li, *Polym. Chem.*, 2018, **9**, 3762–3773.
- L. Wang, K. Zhu, W. Cao, C. Sun, C. Lu and H. Xu, *Polym. Chem.*, 2019, **10**, 2039–2046.
- C. Sun, L. Wang, B. Xianyu, T. Li, S. Gao and H. Xu, *Biomaterials*, 2019, **225**, 119514.
- L. Wang, W. Cao and H. Xu, *ChemNanoMat*, 2016, **2**, 479–488.
- L. Wang, W. Wang, W. Cao and H. Xu, *Polym. Chem.*, 2017, **8**, 4520–4527.
- W. Cao, Y. Gu, T. Li and H. Xu, *Chem. Comm.*, 2015, **51**, 7069–7071.
- F. Fan, S. Gao, S. Ji, Y. Fu, P. Zhang and H. Xu, *Mater. Chem. Front.*, 2018, **2**, 2109–2115.
- M. S. Shim and Y. Xia, *Angew. Chem. Int. Ed.*, 2013, **52**, 6926–6929.

- 35 L. Xu, M. Zhao, W. Gao, Y. Yang, J. Zhang, Y. Pu and B. He, *Colloids Surf. B*, 2019, **181**, 252–260.
- 36 Y. Zhang, J. Zhou, S. Ma, Y. He, J. Yang and Z. Gu, *Biomacromolecules*, 2019, **20**, 1899–1913.
- 37 G.-Q. Lin, W.-J. Yi, Q. Liu, X.-J. Yang and Z.-G. Zhao, *Molecules*, 2018, **23**, 2061.
- 38 P. Pei, C. Sun, W. Tao, J. Li, X. Yang and J. Wang, *Biomaterials*, 2019, **188**, 74–82.
- 39 W. Zhang, X. Hu, Q. Shen and D. Xing, *Nat. Commun.*, 2019, **10**, 1704.
- 40 S. Wang, G. Yu, Z. Wang, O. Jacobson, L.-S. Lin, W. Yang, H. Deng, Z. He, Y. Liu, Z.-Y. Chen and X. Chen, *Angew. Chem. Int. Ed.*, 2019, **58**, 14758–14763.
- 41 A. Stubelius, S. Lee and A. Almutairi, *Acc. Chem. Res.*, 2019, **52**, 3108–3119.
- 42 S. Lee, A. Stubelius, J. Olejniczak, H. Jang, V. A. N. Huu and A. Almutairi, *Biomater. Sci.*, 2018, **6**, 107–114.
- 43 P.-H. Hsu, C. Arboleda, A. Stubelius, L.-W. Li, J. Olejniczak and A. Almutairi, *Biomater. Sci.*, 2020, **8**, 2394–2397.
- 44 S. Lee, A. Stubelius, N. Hamelmann, V. Tran and A. Almutairi, *ACS Appl. Mater. Interfaces*, 2018, **10**, 40378–40387.
- 45 E. Jäger, V. Sincari, L. J. C. Albuquerque, A. Jäger, J. Humajova, J. Kucka, J. Pankrac, P. Paral, T. Heizer, O. Janouskova, R. Konefał, E. Pavlova, O. Sedlacek, F. C. Giacomelli, P. Pouckova, L. Sefc, P. Stepanek and M. Hruby, *Biomacromolecules*, 2020, **21**, 1437–1449.
- 46 E. A. Garcia, D. Pessoa and M. Herrera-Alonso, *Soft Matter*, 2020, **16**, 2473–2479.
- 47 M. E. Anderson, *Chem. Biol. Interact.*, 1998, **111**, 1–14.
- 48 J. M. Estrela, A. Ortega and E. Obrador, *Crit. Rev. Clin. Lab. Sci.*, 2006, **43**, 143–181.
- 49 A. Bansal and M. C. Simon, *J. Cell Biol.*, 2018, **217**, 2291–2298.
- 50 V. P. Bajic, C. V. Neste, M. Obradovic, S. Zafirovic, D. Radak, V. B. Bajic, M. Essack and E. R. Isenovic, *Oxid. Med. Cell. Longev.*, 2019, **2019**, 5028181.
- 51 G. K. Balendiran, R. Dabur and D. Fraser, *Cell Biochem. Funct.*, 2004, **22**, 343–352.
- 52 J. F. Quinn, M. R. Whittaker and T. P. Davis, *Polym. Chem.*, 2017, **8**, 97–126.
- 53 R. R. Perry, J. A. Mazetta, M. Levin and S. C. Barranco, *Cancer*, 1993, **72**, 783–787.
- 54 A. E. Oberli-Schrämmli, F. Joncourt, M. Stadler, H. J. Altermatt, K. Buser, H. B. Ris, U. Schmid and T. Cerny, *Int. J. Cancer*, 1994, **59**, 629–636.
- 55 Y. Soini, U. Näpänkangas, K. Järvinen, R. Kaarteenaho-Wiik, P. Pääkkö and V. L. Kinnula, *Cancer*, 2001, **92**, 2911–2919.
- 56 A. Seven, Y. Erbil, R. Seven, F. Inci, T. Gülyaşar, B. Barutçu and G. Candan, *Cancer Biochem. Biophys.*, 1998, **16**, 333–345.
- 57 N. Traverso, R. Ricciarelli, M. Nitti, B. Marengo, A. L. Furfaro, M. A. Pronzato, U. M. Marinari and C. Domenicotti, *Oxid. Med. Cell. Longev.*, 2013, **2013**, 972913.
- 58 M. P. Gamcsik, M. S. Kasibhatla, S. D. Teeter and O. M. Colvin, *Biomarkers*, 2012, **17**, 671–691.
- 59 G. K. Balendiran, R. Dabur and D. Fraser, *Cell Biochem. Funct.*, 2004, **22**, 343–352.
- 60 M. H. Lee, Z. Yang, C. W. Lim, Y. H. Lee, S. Dongbang, C. Kang and J. S. Kim, *Chem. Rev.*, 2013, **113**, 5071–5109.
- 61 J. K. Oh, *Polym. Chem.*, 2019, **10**, 1554–1568.
- 62 R. Bej, P. Dey and S. Ghosh, *Soft Matter*, 2020, **16**, 11–26.
- 63 K. K. Bawa, A. M. Jazani, C. Shetty and J. K. Oh, *Macromol. Rapid Commun.*, 2018, **39**, 1800477.
- 64 P. Ju, J. Hu, F. Li, Y. Cao, L. Li, D. Shi, Y. Hao, M. Zhang, J. He and P. Ni, *J. Mater. Chem. B*, 2018, **6**, 7263–7273.
- 65 H. Hu, J. Wan, X. Huang, Y. Tang, C. Xiao, H. Xu, X. Yang and Z. Li, *Nanoscale*, 2018, **10**, 10514–10527.
- 66 X. Du, Y. Sun, M. Zhang, J. He and P. Ni, *ACS Appl. Mater. Interfaces*, 2017, **9**, 13939–13949.
- 67 B. Saha, S. Bhattacharyya, S. Mete, A. Mukherjee and P. De, *ACS Appl. Polym. Mater.*, 2019, **1**, 2503–2515.
- 68 J. Tan, Z. Deng, G. Liu, J. Hu and S. Liu, *Biomaterials*, 2018, **178**, 608–619.
- 69 X. Hu, J. Hu, J. Tian, Z. Ge, G. Zhang, K. Luo and S. Liu, *J. Am. Chem. Soc.*, 2013, **135**, 17617–17629.
- 70 C. M. Hu and L. Zhang, *Biochem. Pharmacol.*, 2012, **83**, 1104–1111.
- 71 J. Shen, Q. Wang, J. Fanga, W. Shen, D. Wu, G. Tang and J. Yan, *RSC Adv.*, 2019, **9**, 37232–37240.
- 72 G. Biswas, B. C. Jena, S. Sahoo, P. Samanta, M. Mandal and D. Dhara, *Green Chem.*, 2019, **21**, 5624–5638.
- 73 K. Bhattacharya, S. L. Banerjee, S. Das, S. Samanta, M. Mandal and N. K. Singha, *ACS Appl. Bio Mater.*, 2019, **2**, 2587–2599.
- 74 L. Li, D. Li, M. Zhang, J. He, J. Liu and P. Ni, *Bioconjugate Chem.*, 2018, **29**, 2806–2817.
- 75 Y. Zhao, C. Simon, M. D. Attieh, K. Haupt and A. Falcimaigne-Cordin, *RSC Adv.*, 2020, **10**, 5978–5987.
- 76 M. N. Hughes, M. N. Centelles and K. P. Moore, *Free Radic. Biol. Med.*, 2009, **47**, 1346–1353.
- 77 C. Szabo, *Biochem. Pharmacol.*, 2018, **149**, 5–19.
- 78 D. Benchoam, E. Cuevasanta, M. N. Möller and B. Alvarez, *Antioxidants*, 2019, **8**, 48.
- 79 D. J. Elsey, R. C. Fowkes and G. F. Baxter, *Cell Biochem. Funct.*, 2010, **28**, 95–106.
- 80 M. R. Filipovic, J. Zivanovic, B. Alvarez and R. Banerjee, *Chem. Rev.*, 2018, **118**, 1253–1337.
- 81 J. L. Wallace, *Trends Pharmacol. Sci.*, 2007, **28**, 501–505.
- 82 Y. C. Wu, X. J. Wang, L. Yu, F. K. L. Chan, A. S. L. Cheng, J. Yu, J. Y. Sung, W. K. K. Wu and C. H. Cho, *PLoS One*, 2012, **7**, e37572.
- 83 P. Rose, P. K. Moore and Y. Z. Zhu, *Cell. Mol. Life Sci.*, 2017, **74**, 1391–1412.
- 84 B. D. Paul and S. H. Snyder, *Biochem. Pharmacol.*, 2018, **149**, 101–109.
- 85 Y. Shen, Z. Shen, S. Luo, W. Guo and Y. Z. Zhu, *Oxid. Med. Cell. Longev.*, 2015, **2015**, 925167.
- 86 L.-L. Pan, M. Qin, X.-H. Liu and Y.-Z. Zhu, *Front. Pharmacol.*, 2017, **8**, 686.
- 87 X. Cao, L. Ding, Z.-Z. Xie, Y. Yang, M. Whiteman, P. K. Moore and J.-S. Bian, *Antioxid. Redox Signal.*, 2019, **31**, 1–38.
- 88 M. R. Hellmich and C. Szabo, *Handb. Exp. Pharmacol.*, 2015, **230**, 233–241.
- 89 W. Chen, Y. Zhang, X. Li, H. Chen, J. Sun and F. Feng, *ACS Appl. Mater. Interfaces*, 2017, **9**, 33571–33575.
- 90 N. Thirumalaivasan, P. Venkatesan, P.-S. Lai and S.-P. Wu, *ACS Appl. Bio Mater.*, 2019, **2**, 3886–3896.
- 91 V. S. Lin, W. Chen, M. Xian and C. J. Chang, *Chem. Soc. Rev.*, 2015, **44**, 4596–4618.
- 92 X. Wang, L. An, Q. Tian and K. Cui, *RSC Adv.*, 2019, **9**, 33578–33588.
- 93 H. A. Henthorn and M. D. Pluth, *J. Am. Chem. Soc.*, 2015, **137**, 15330–15336.
- 94 Q. Yan and W. Sang, *Chem. Sci.*, 2016, **7**, 2100–2105.
- 95 H. Zhang, X. Kong, Y. Tang and W. Lin, *ACS Appl. Mater. Interfaces*, 2016, **8**, 16227–16239.
- 96 P.-H. Hsu, R. Kawasaki, K. Yamana, H. Isozaki, S. Kawamura, A. Ikeda and A. Almutairi, *ACS Appl. Polym. Mater.*, 2020, **2**, 3756–3760.
- 97 W. Yin, W. Ke, N. Lu, Y. Wang, A. A.-W. M. M. Japir, F. Mohammed, Y. Wang, Y. Pan and Z. Ge, *Biomacromolecules*, 2020, **21**, 921–929.
- 98 H. Xu, W. Cao and X. Zhang, *Acc. Chem. Res.*, 2013, **46**, 1647–1658.
- 99 B. Z. Hailemeskel, K. D. Addisu, A. Prasannan, S. L. Mekuria, C.-Y. Kao and H.-C. Tsai, *Appl. Surf. Sci.*, 2018, **449**, 15–22.
- 100 Y. Tian, M. Lei, L. Yan and F. An, *Polym. Chem.*, 2020, **11**, 2360–2369.

## ARTICLE

## Journal Name

- 101 L. Zhang, Y. Liu, K. Zhang, Y. Chen and X. Luo, *Colloid Polym. Sci.*, 2019, **297**, 225–238.
- 102 B. Sun, C. Luo, X. Zhang, M. Guo, M. Sun, H. Yu, Q. Chen, W. Yang, M. Wang, S. Zuo, P. Chen, Q. Kan, H. Zhang, Y. Wang, Z. He and J. Sun, *Nat. Commun.*, 2019, **10**, 3211.
- 103 P. Cheng and K. Pu, *ACS Appl. Mater. Interfaces*, 2020, **12**, 5286–5299.
- 104 C. Wang, S. Ding, S. Wang, Z. Shi, N. K. Pandey, L. Chudal, L. Wang, Z. Zhang, Y. Wen, H. Yao, L. Lin, W. Chen and L. Xiong, *Coord. Chem. Rev.*, 2021, **426**, 213529.